JACS
JOURNAL OF THE AMERICAN CHEMICAL SOCIETY

Communication

pubs.acs.org/JACS

Synthesis and Alignment of Discrete Polydiacetylene-Peptide Nanostructures

Stephen R. Diegelmann,[†,‡,§,⊥] Nikolaus Hartman,[§,∥] Nina Markovic,[§,∥] and John D. Tovar*[,†,‡,§]

[†]Department of Chemistry, [‡]Department of Materials Science and Engineering, [§]Institute for NanoBioTechnology, and [∥]Department of Physics and Astronomy, Johns Hopkins University, 3400 North Charles Street, Baltimore, Maryland 21218, United States

Supporting Information

ABSTRACT: Oligopeptides bearing internal diacetylene units are shown to self-assemble in water into one-dimensional nanostructures and aligned macroscopic hydrogels. The diacetylene units can be photopolymerized into polydiacetylenes that run coincident to the nanostructure and noodle long axes, and the resulting nanostructures show evidence for ambipolar charge transport. This self-assembly, alignment and polymerization technique provides a rapid way to produce globally aligned collections of conjugated polymer chains.

Uniformly aligned macroscopic assemblies of individual π-conjugated polymers or nanoscale fibrils thereof, as opposed to the microscale domains commonly found in thin films of crystalline organic semiconductive polymers, would offer many opportunities for nanotechnology. We report how short oligopeptides bearing internal diacetylenes (DA) self-assemble into amyloid-like nanomaterials that can be aligned via a simple solution dispensing process and subsequently photopolymerized into polydiacetylene (PDA) nano- and macrostructures. These PDA–peptide structures are water processable, manipulatable, and (for the macrostructures) consist of globally aligned individual bundles of isolated conjugated polymers. Unique to this work are demonstrations of chemically driven chromic alteration and gate-induced carrier formation within nanostructures arising from PDAs derived from unusual topochemical polymerizations of diarylbutadiynes. Oligomeric π-electron materials have been incorporated directly into the backbones of organo-[1] and water-soluble[2−5] peptides leading to intermolecular electronic delocalization within self-assembled one-dimensional (1D) nanostructures, but this is the first report to use simple water-soluble peptides embedded with reactive chromophores to prepare aligned intramolecular electronic conduits of conjugated polymers.

PDAs have received considerable attention following the pioneering demonstration by Wegner that crystalline DAs with specific intermolecular geometric constraints can undergo topochemical polymerization to form PDAs.[6] Several material systems have encouraged PDA formation, from single crystals[7,8] to self-assembled monolayers and vesicles.[9,10] There have only been a few examples of PDA formation within 1D nanostructures under organic[11] or aqueous environments,[12−14] but the PDAs thus formed (e.g., those within peptide amphiphile nanofiber matrices) are bundled collections of multiple polymer chains. Our design incorporates the DA units directly within the backbones of water-soluble oligopeptides and directs the formation of electronically delocalized 1D amyloid-like nanostructures, including those that are comprised of single PDA conjugated chains. Biologically compatible 1D "wires" would provide important advances for bioelectronics.

We prepared several peptide–DA–peptide molecules to explore their self-assembly, topochemical polymerization, and alignment. We subjected α,ω-diacid DAs **1**[15] and **2**[16] to solid-phase dimerization reactions developed in our lab for the incorporation of π-electron units into short oligopeptide chains.[4] Using the aliphatic diacid **1**, we prepared peptide **3**, and the aromatic diacid **2** led to peptides **4** and **5** (Figure 1).[17]

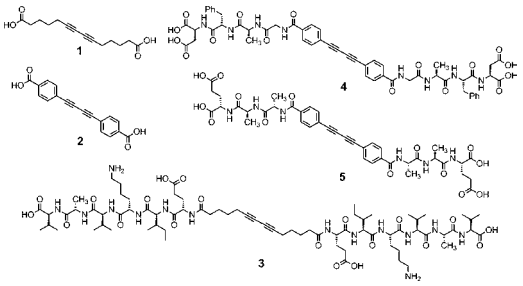

Figure 1. Molecular structures of DA diacids and peptides.

Peptide **3** was soluble at basic pH and formed a self-supporting hydrogel under more acidic pH, a common indicator for these types of materials that suggests molecular self-assembly into 1D nanostructures. Unfortunately, UV irradiation of the peptide nanostructures formed from **3** did not produce PDA. Analysis of the light irradiated product indicated the formation of a hydrolyzed yne-one [Figure S11, Supporting Information (SI)]. This suggests that the DA units are either exposed to water during irradiation or that the flexibility of the butyl spacers prevents polymerization.[15]

Nanostructures comprised of diphenyl DAs **4** and **5** placed the reactive diynes in proper position to allow for successful topochemical polymerizations (Figure S18, SI). This is remarkable because there are very few reports of successful diphenyl DA polymerizations.[18−21] The peptide assembly energetics thus override unfavorable steric or quadrupole stacking within the nanostructures while affording a dynamic environment to promote cross-linking. The nanostructures obtained after assembly of **4** were dispersed in water and

Received: December 9, 2011
Published: January 10, 2012

irradiated with UV light (254 nm) and the formation of PDA monitored by absorption spectroscopy (Figure 2b). The low-

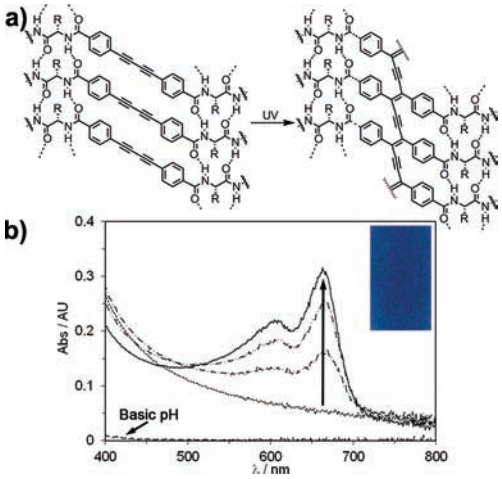

Figure 2. (a) Stacked DA peptides (right) and resulting PDA. (b) UV–vis spectra taken after continual UV irradiation of **4** in acidic solution (at 0, 0.5, 5, and 20 min intervals). The spectrum recorded at basic pH is indicated on the graph.[17] Inset: Film of an assembled solution of peptide **4** cast onto a glass slide (~ 3 cm^2) followed by irradiated with UV light for 30 min to form blue PDA.

energy absorption bands (λ_{abs} = 663, 606 nm) and visible blue color after irradiation indicated PDA formation. This polymerization occurred in solution and in the solid state as a drop cast film (inset in Figure 2b). The absorption bands indicate a very high degree of planarity and conjugation throughout the PDA backbone relative to other reported diphenyl DA polymerizations. Irradiation of **5** was accompanied by the formation of a yellow solution, indicative of DA oxidation, in addition to blue PDA. The relatively less hydrophobic EAA sequence of **5** promotes the formation of smaller nanostructures that expose more DA units to the aqueous media.[22] There is a clear balance needed between structures large enough to bury the DA units from water while being small enough to prevent aggregates from precipitating out of solution. Sterically demanding sequences can also foster polymerization as observed with biotin-containing DA peptides (SI). In all cases, the long axes of the PDA chains can be envisioned to run coincident with the length of the 1D amyloid-like nanostructures.

The hydrogen-bonding networks within the PDA nanostructures were disrupted by raising the pH and inducing charge repulsion among the resulting carboxylates that forced the PDA chains to adopt less planar conformations (Figure S19, SI). This disruption led to a blue shift in the low-energy PDA UV–vis absorptions and a visual color change from blue (602, 558 nm) to reddish purple (592, 543 nm) (Figure 3a). Likewise, the circular dichroism (CD) spectra of the PDA nanostructures showed intense signals (345, 368 nm) with a weak excitonic Cotton effect at lower energy (Figure 3b). These CD signals were dramatically diminished upon raising the pH (pH ~ 8). Reacidification of the solution then recovered the initial UV–vis and CD spectral signatures, indicating that the local planarity and chirality of the polymer chromophores enforced by β-sheet hydrogen bonding were re-established. These switching responses establish that the peptide–PDA nanomaterial conjugation is responsive to environmental stimuli, and

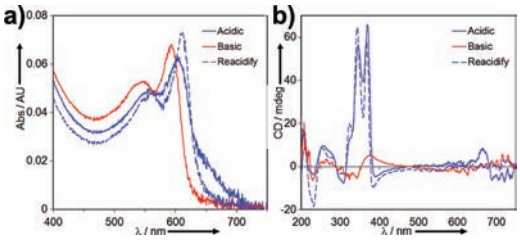

Figure 3. (a) UV–vis spectra of polymerized **5** in acidic (pH ~ 2, solid blue), basic (pH ~ 8, red), and reacidified (pH ~ 2, dashed blue) aqueous solution. (b) CD spectra of polymerized **4** in acidic (solid blue), basic (red), and reacidified (dashed blue) 1:1 water/ethanol solution.

our future work will address more biologically relevant detection scenarios[23] (e.g., with biotin-mediated binding, SI).

The nanostructures formed from **4** and **5** were examined with AFM. Peptide **4** was dissolved in basic water (pH 7–8) to form a clear solution (up to 10 mg/mL or 9.3 mM). The acidification of that solution resulted in an opaque gel that slowly formed macroscopic aggregates over approximately 5 min. Although we could observe 1D nanomaterials by diluting this gel and imaging by atomic force microscopy (AFM), visualization was difficult due to the presence of larger aggregates (Figure S12, SI). Despite their water solubility, we found that the addition of ethanol (1:1 v/v with water) prior to the assembly led to better dispersion of the nanomaterials presumably through better wetting of the substrate. In all cases, the assembled solutions were polymerized with a hand-held UV lamp prior to sample deposition and imaging by AFM. Peptide **4** assembled into nanostructures with diameters ranging from larger 30–40 nm bundles down to smaller branched 3–5 nm structures (Figure 4). The hydrophobicity of the DFAG

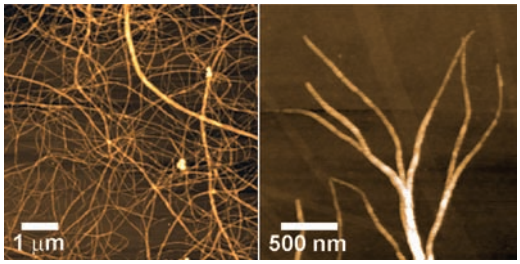

Figure 4. AFM images of PDA nanostructures derived from peptide **4** on SiO_2 substrates.

tetrapeptide sequence in **4** promotes hierarchical aggregation beyond that of single β-sheet tapes as to be expected for an amyloid-like assembly process. The less hydrophobic EAA tripeptide sequence in **5** limited this process to individual and better-dispersed nanostructures rather than the larger diameter objects (Figure S13, SI). These AFM images depict bundled PDA chains as well as what we believe to be the first examples of single PDA chains embedded within discrete nanostructures (Figure 4, left panel).

Electrostatic force microscopy (EFM) was used to probe the electronic behavior of the PDA core inside the peptide nanostructures. This technique uses an AFM to first collect the height profile in tapping mode. The measured height profile is then used in the second scan in order to maintain the tip at a constant height above the sample, while applying a constant voltage between the tip and the sample, analogous to gating a

dx.doi.org/10.1021/ja211539j | J. Am. Chem.Soc. 2012, 134, 2028–2031

field effect transistor. Electrostatic force between the tip and the sample shifts the phase of the oscillation of the tip, allowing the measurement of the electrostatic force gradient as a function of the tip position. This technique has been used to differentiate between conductive carbon nanotubes (CNTs) and insulating λ-DNA nanostructures on SiO_2 surfaces.[24] The height profiles are comparable to those found in standard AFM (3−15 nm, Figure S14, SI). EFM images of dispersed peptide−PDA nanostructures were obtained for a range of tip voltages from −5 to +5 V to probe the response of the charge carriers to the electric field over the length of the nanostructures (Figure 5). It

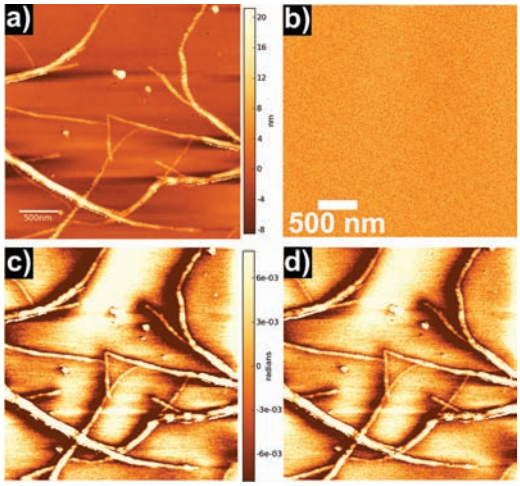

Figure 5. EFM images showing the (a) topography and phase shift images of peptide−PDA nanostructures from peptide **4** (b) without an applied tip voltage and with (c) −5 and (d) + 5 V applied to the tip.

is clear that in the absence of tip voltage (Figure 5b), there is no tip/fiber interaction indicating no electric field in the nanostructure. The observed phase shift images and their dependence on the tip voltage (Figure 5c,d) indicate that charge carriers can be induced within these structures that move freely over their lengths despite the presence of the peptides.

The phase shift images for both negative and positive tip voltage show distinct 'negative−positive−negative' contrast across the short axis of each individual structure. This contrast has been observed in other organic conducting nanofibers and is thought to arise from the difference in the capacitance of the system as the tip scans over the nanofiber: a horizontal attractive force is felt by the tip as it approaches the side of the nanofiber, followed by a repulsive force when the tip travels directly above it.[25]

The present peptide−PDA assemblies are comprised of randomly oriented 1D nanostructures. There are many known techniques to align π-conjugated polymers or self-assembled nanostructures,[26] including those that use physical rubbing,[27] Langmuir−Blodgett films,[28] extrusion from mesoporous inorganic crystals,[29] the addition of small molecules such as liquid crystals,[30] "aligner"[31] and "twimer"[32] compounds, and the application of strong electric[30] or magnetic fields.[12] More recently, we employed a solution dispensing route first reported by Stupp[33] to achieve macroscopic (cm scale) domains of aligned π-conjugated peptide nanostructures within physically manipulatable "noodle-like" hydrogels.[34] This method is attractive when compared to the above techniques because it is performed completely in aqueous media using an experimentally simple technique. We thus reasoned that we could effect alignment of conjugated polymers for intramolecular delocalization provided that DA-based peptide noodles could also undergo topochemical polymerization.

Scanning electron microscopy (SEM) shows the random network formation usually observed for self-assembled peptide hydrogels (Figure 6a). SEM of a peptide hydrogel formed using

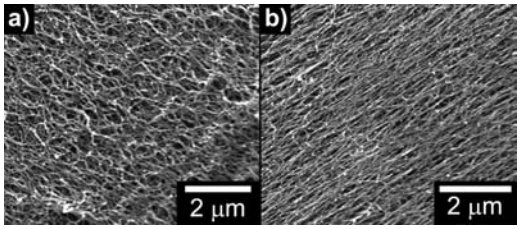

Figure 6. SEM images of polymerized gel of peptide **4** as an unaligned hydrogel (a) and as an aligned peptide noodle (b).

the extrusion technique revealed globally aligned peptide−DA nanostructures within macroscopic noodles (Figure 6b). Although Figure 6b shows an area of ca. 44 μm^2, comparable alignment can be envisioned throughout the macroscopic structure (mm−cm scales). These noodle macrostructures were subjected to UV irradiation leading to the formation of blue hydrogel noodles (Figure 7a), a color that was observed above

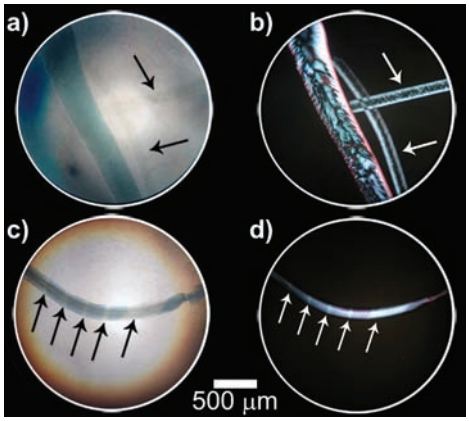

Figure 7. Peptide **4** hydrogel noodles before (colorless) and after (blue) DA polymerization as seen under a light microscope (a) without and (b) with crossed polarizers. Spatially controlled polymerization of a peptide−DA noodle performed by shielding with a TEM grad shadow mask (c, d). Arrows indicate regions shielded from UV light.

during the polymerization of randomly aligned peptide−DA nanostructures. The present system thus offers an experimentally facile method to align peptide nanostructures poised for topochemical polymerization to yield highly aligned arrays of conjugated polymers within nanostructured 1D fibrils, all available from one simple solution manipulation.

Polarized optical microscopy (POM) was used investigate the extent of global alignment of the peptide−PDA noodles as well as differentiate between the birefringence before and after polymerization (Figure 7b). Although both samples are birefringent, there is a clear color contrast in the polymerized material leading to a reddish appearance. This color is not associated with a resonant process but reflects how the nanostructures within the noodles interact with the polarized

light. Spatially resolved PDA formation along the length of the peptide−DA noodle was achieved by using a TEM grid as a shadow mask during the photopolymerization (Figure 7c,d). PDA formation only occurred where the shadow mask allowed the transmission of the UV light. When viewed with POM, the locations with and without PDA formation are clearly visible as areas of different color and birefringence. This spatially resolved polymerization produces 'microbarcodes' and could be used to prepare electronic or mechanical gradients throughout a macroscopic noodle made up of aligned conjugated polymers.

Self-assembling nanostructures with polymerizable units provide new and unique ways to further the development of electronic nanomaterials. The thermodynamic equilibria associated with molecular self-assembly processes render them dynamic and reversible, and they could be disassembled under suitable stimuli, whether intentional or not. The PDA-based nanofibers presented here allow for postassembly manipulation while maintaining the supramolecular structure through intermolecular covalent links formed during polymerization. The extrusion alignment technique provides a facile way to access aligned conjugated polymers without the use of physical 'director' influences or the application of external fields. The hydrogel noodles described here are made up of globally aligned π-conjugated peptide−PDA polymers that have ambipolar semiconductor properties, and such manipulatable aligned macrostructures could be useful in future research to directly interface functional nanomaterials with common solid-state devices and biological systems.

■ ASSOCIATED CONTENT

Supporting Information

Experimental, characterization, and instrumental details, and additional UV−vis and AFM images. This material is available free of charge via the Internet at http://pubs.acs.org.

■ AUTHOR INFORMATION

Corresponding Author

tovar@jhu.edu

Present Address

[⊥]Macromolecular Science and Engineering, Case Western Reserve University, 2100 Adelbert Road, Cleveland, Ohio 44106, United States.

■ ACKNOWLEDGMENTS

We thank Dr. J. Michael McCaffery (JHU IIC) and Ms. Julie Bitter for help acquiring and interpreting POM images. S.R.D. was an NSF-IGERT Fellow through JHU's INBT. We thank Johns Hopkins University, JHU's Institute for NanoBioTechnology, the National Science Foundation (DMR-1106167, N.M.), and the Department of Energy Office of Basic Energy Sciences (DE-SC0004857, J.D.T. peptide nanomaterials) for generous support.

■ REFERENCES

(1) Schillinger, E. K.; Mena-Osteritz, E.; Hentschel, J.; Börner, H. G.; Bäuerle, P. *Adv. Mater.* **2009**, *21*, 1562.

(2) Diegelmann, S. R.; Gorham, J. M.; Tovar, J. D. *J. Am. Chem. Soc.* **2008**, *130*, 13840.

(3) Stone, D. A.; Hsu, L.; Stupp, S. I. *Soft Matter* **2009**, *5*, 1990.

(4) Vadehra, G. S.; Wall, B. D.; Diegelmann, S. R.; Tovar, J. D. *Chem. Commun.* **2010**, *46*, 3947.

(5) Mba, M.; Moretto, A.; Armelao, L.; Crisma, M.; Toniolo, C.; Maggini, M. *Chem.—Eur. J.* **2011**, *17*, 2044.

(6) Wegner, G. Z. *Naturforscher.* **1969**, *24* (b), 824. Wegner, G. *J. Polym. Sci., Polym. Lett. Edn.* **1971**, *9*, 133. Wegner, G. *Pure Appl. Chem.* **1977**, *49*, 443.

(7) Xu, Y.; Smith, M.; Geer, M.; Pellechia, P.; Brown, J.; Wibowo, A.; Shimizu, L. *J. Am. Chem. Soc.* **2010**, *132*, 5334.

(8) Sun, A.; Lauher, J.; Goroff, N. *Science* **2006**, *312*, 1030.

(9) Huo, Q.; Wang, S.; Pisseloup, A.; Verma, D.; Leblanc, R. *Chem. Commun.* **1999**, *16*, 1601.

(10) Biesalski, M.; Tu, R.; Tirrell, M. V. *Langmuir* **2005**, *21*, 5663.

(11) Jahnke, E.; Lieberwirth, I.; Severin, N.; Rabe, J. P.; Frauenrath, H. *Angew. Chem., Int. Ed.* **2006**, *45*, 5383.

(12) Löwik, D. W. P. M; Shklyarevskiy, I. O.; Ruizendaal, L.; Christianen, P. C. M.; Maan, J. C.; van Hest, J. C. M. *Adv. Mater.* **2007**, *19*, 1191.

(13) Hsu, L.; Cvetanovich, G. L.; Stupp, S. I. *J. Am. Chem. Soc.* **2008**, *130*, 3892.

(14) Stone, D. A.; Hsu, L.; Wheeler, N. R.; Wilusz, E.; Zukas, W.; Wnek, G. E.; Korley, L. T. J. *Soft Matter.* **2011**, *7*, 2449.

(15) Aoki, K.; Kudo, M.; Tamaoki, N. *Org. Lett.* **2004**, *6*, 4009.

(16) Matsubara, H.; Shimura, T.; Hasegawa, A.; Semba, M.; Asano, K.; Yamamoto, K. *Chem. Lett.* **1998**, *27*, 1099.

(17) For experimental details, see Supporting Information.

(18) Sarkar, A.; Okada, S.; Matsuzawa, H.; Matsudab, H.; Nakanishi, H. *J. Mater. Chem.* **2000**, *10*, 819.

(19) Matsuo, H.; Okada, S.; Nakanishi, H.; Matsuda, H.; Takaragi, S. *Polym. J.* **2002**, *34*, 825.

(20) Chan, Y-H; Lin, J-T; Chen, I-W P.; Chen, C.-H. *J. Phys. Chem. B.* **2005**, *109*, 19161.

(21) Néabo, J.; Tohoundjona, K.; Morin, J. *Org. Lett.* **2011**, *13*, 1358.

(22) Aggeli, A.; Nyrkova, I. A.; Bell, M.; Harding, R.; Carrick, L.; McLeish, T. C.; Semenov, A. N.; Boden, N. *Proc. Natl. Acad. Sci. U.S.A.* **2001**, *98*, 11857.

(23) Charych, D. H.; Nagy, J. O.; Spevak, W.; Bednarski, M. D. *Science* **1993**, *261*, 585.

(24) Bockrath, M.; Markovic, N.; Shepard, A.; Tinkham, M.; Gurevich, L.; Kouwenhoven, L. P.; Wu, M. W.; Sohn, L. L. *Nano Lett.* **2002**, *2*, 187.

(25) Staii, C.; Johnson, A. T.; Pinto, N. J. *Nano Lett.* **2004**, *4*, 859.

(26) Methods for aligning conjugated polymers see: *Semiconducting Polymers Applications, Properties, and Synthesis (ACS Symposium)*; Hsieh, B. R. , Wei, Y., Eds; American Chemical Society: Washington, DC, 1999; p 735.

(27) Heil, H.; Finnberg, T.; von Malm, N.; Schmechel, R.; von Seggern, H. *J. App. Phys.* **2003**, *93*, 1636.

(28) Suzuki, M.; Ferencz, A.; Iida, S.; Enkelmann, V.; Wegner, G. *Adv. Mater.* **1993**, *5*, 359.

(29) Tajima, K.; Aida, T. *Chem. Commun.* **2000**, *24*, 2399.

(30) Zhu, Z.; Swager, T. M. *J. Am. Chem. Soc.* **2002**, *124*, 9670.

(31) Kubo, Y.; Kitada, Y.; Wakabayashi, R.; Kishida, T.; Ayabe, M.; Kaneko, K.; Takeuchi, M.; Shinkai, S. *Angew. Chem., Int. Ed.* **2006**, *45*, 1548.

(32) Takeuchi, M.; Fujikoshi, C.; Kubo, Y.; Kaneko, K.; Shinkai, S. *Angew. Chem., Int. Ed.* **2006**, *45*, 5494.

(33) Zhang, S.; Greenfield, M. A.; Mata, A.; Palmer, L. C.; Bitton, R.; Mantei, J. R.; Aparicio, C.; de la Cruz, M. O.; Stupp, S. I. *Nat. Mater.* **2010**, *9*, 594.

(34) Wall, B. D.; Diegelmann, S. R.; Zhang, S.; Dawidczyk, T. J.; Wilson, W. L.; Katz, H. E.; Mao, H. Q.; Tovar, J. D. *Adv. Mater.* **2011**, *23*, 5009.